

Article

Investigating Vibration Characteristics of Cross-Laminated Timber Panels Made from Fast-Grown Plantation *Eucalyptus nitens* under Different Support Conditions

Yingwei Liang ^{1,2,*} , Assaad Taoum ² , Nathan Kotlarewski ¹ , Andrew Chan ²  and Damien Holloway ² 

¹ Centre for Sustainable Architecture with Wood, University of Tasmania, Launceston, TAS 7250, Australia; nathan.kotlarewski@utas.edu.au

² School of Engineering, College of Sciences and Engineering, University of Tasmania, Hobart, TAS 7001, Australia; assaad.taoum@utas.edu.au (A.T.); andrew.chan@utas.edu.au (A.C.); damien.holloway@utas.edu.au (D.H.)

* Correspondence: yingwei.liang@utas.edu.au

Abstract: The mechanical properties of fibre-managed *Eucalyptus nitens* (*E. nitens*) cross-laminated timber (CLT) have previously been extensively studied, proving the material to be structurally safe and reliable. However, the vibration performance of CLT manufactured from this relative new construction species is not yet fully understood, especially under different support conditions. In this study, three types of support conditions, including roller–roller, bearer–bearer and clamp–bearer support conditions, were examined under vibration impulse-response testing performed using a simple but effective and repeatable excitation method consisting of a basketball dropped from a known height and an accelerometer. Six three-ply *E. nitens* CLT panels considered to have different moduli of elasticity in different layers and one strength-class C24 spruce CLT as a controlled reference were included in this study. The results suggest that the fundamental frequency values can effectively reflect the inherent characteristics of CLT panels (bending stiffness and density); however, no obvious relationship was observed between damping ratios and these inherent properties. The values of frequency constant λ_1 were determined to analyse the effect of different support conditions on the values of fundamental frequency. The average values of λ_1 for the roller–roller (9.6) and bearer–bearer (10.1) supports align with the theoretical values (9.87) for simply support (S-S) conditions. However, when clamping loads were applied at one edge of the bearer support, the average values of λ_1 increased up to 10.8 but remained far below the theoretical values for clamped–pinned (C-S) support (15.4).

Keywords: hardwood cross-laminated timber; vibration; fibre-managed *Eucalyptus nitens*; serviceability performance



Citation: Liang, Y.; Taoum, A.; Kotlarewski, N.; Chan, A.; Holloway, D. Investigating Vibration Characteristics of Cross-Laminated Timber Panels Made from Fast-Grown Plantation *Eucalyptus nitens* under Different Support Conditions. *Buildings* **2024**, *14*, 831. <https://doi.org/10.3390/buildings14030831>

Academic Editor: Paulo Cachim

Received: 17 January 2024

Revised: 8 March 2024

Accepted: 14 March 2024

Published: 19 March 2024



Copyright: © 2024 by the authors. Licensee MDPI, Basel, Switzerland. This article is an open access article distributed under the terms and conditions of the Creative Commons Attribution (CC BY) license (<https://creativecommons.org/licenses/by/4.0/>).

1. Introduction

According to Australian plantation statistics and the log availability report (ABARES) in 2021 [1], Tasmania accounts for approximately 35% of national hardwood availability, dominating the national supply of both pulp and sawlogs for Australia. The main hardwood species among this log availability in Tasmania is *E. nitens*, and most of these plantations are fibre-managed and used to produce woodchips. Nevertheless, the large quantities have raised a lot of interest in utilising these raw materials to produce wood products for the building industry. In order to achieve this, a number of challenges need to be overcome. One of the most important challenges is to accurately grade *E. nitens* feedstock for structural applications. Typical grading methods based on visual grading have proven to be inaccurate [2] due to the large number of strength-reducing features (SRFs) such as knots. Balasso et al. [3] and Ettelaie et al. [4] have conducted successful studies using machine-stress grading, acoustic wave velocity (AWV) and linear–elastic

four-point bending tests to accurately determine and predict the grade of *E. nitens* sawn boards. This represents the first step in understanding the potential of utilising this material in mass-laminated timber manufacturing, such as cross-laminated timber (CLT).

Cross-laminated timber (CLT) is one option for utilising fibre-managed *E. nitens* feedstocks because the orthogonal layup can potentially offer more uniform physical and mechanical properties and reduce the effect of individual SPFs [5]. Pangh et al. [6] conducted pioneering research to determine the bending properties of CLT derived from *Eucalyptus* plantations. Their findings, including the modulus of elasticity (MOE) and modulus of rupture (MOR), suggested the potential utilisation of *Eucalyptus* plantations in CLT applications. Subsequently, Ettelaei et al. [5] investigated rolling shear properties on heterogeneous *E. nitens* CLT samples under the Planar Shear Test. The results demonstrated that the performance of heterogeneous *E. nitens* CLT was satisfactory. This suggests that there is potential for utilising locally sourced timber species in Tasmania for the production of highly structurally efficient CLT panels. The findings from these studies have laid the groundwork for the use of Australian plantation hardwood CLT in commercial structural applications. However, the serviceability performance of fibre-managed *E. nitens* CLT, particularly our knowledge of its vibration performance, still remains limited.

The strong in-plane and out-of-plane carrying capacities of CLT allow it to achieve longer spans of flooring in residential and commercial buildings. However, a large span of flooring can potentially result in vibrational issues, which will have a significant impact on human comfort, especially when the fundamental frequencies of the vibration fall within the range of 0–80 Hz [7,8]. Therefore, as the use of CLT in construction continues to increase, there is a compelling need to understand the vibration performance of CLT floors, and this knowledge can help explore methods to improve their serviceability performance and largely mitigate annoying vibrations for occupants. Hu et al. [9] carried out a vibration measurement and subjective evaluation on a CLT floor in laboratory conditions, and they found that the types of joints, the span, the edge supports, the topping and the ceiling have a significant influence on the vibration performance of CLT. The knowledge obtained from this literature source has played an important role in the CLT handbook [10] and standard [11]. Furthermore, Chúláin and Harte [12] investigated the vibration behaviour of CLT floors using methods similar to those of European Standard EN 16929 [13]. They found that the inclusion of support brackets can improve the vibration performance of the CLT floor, while adding mass to the CLT floor did not influence its deflection but significantly reduced the fundamental frequencies. Nevertheless, most of the research on this topic focuses on softwood CLT.

As interest in utilising hardwood CLT has been growing recently, it has become more necessary to investigate the vibration performance of hardwood CLT. Crovella and Kurzinski [14] carried out experimental tests to investigate the vibration performance of hardwood CLT (black locust). They found that hardwood species are easier to use in designing the serviceability of CLT flooring systems due to their more predictable natural frequency. Liang et al. [15] performed the first vibration test on fibre-managed *E. nitens* CLT and demonstrated its superior performance when compared to strength-class C24 [16] spruce CLT. Nevertheless, in order to gain a comprehensive understanding of the vibration performance of *E. nitens* CLT as a flooring system, it is necessary to consider various boundary conditions in further investigations. Accordingly, the primary focus of this study is to explore its vibration performance by examining these essential factors.

It has been shown that boundary conditions are crucial to understanding the vibration response of floors. Theoretically, the natural frequencies of a vibrating system vary based on the total restrained degrees of freedom (DOFs), and the restrained DOFs are related to the boundary conditions of the system [17]. Several works in the literature offer valuable insights into the effect of various boundary conditions on the vibration performance of CLT flooring systems. For example, Chúláin et al. [18] studied the influence of different support conditions on the serviceability response of CLT floors using finite element analysis. Their results revealed that under semi-rigid and fully fixed support conditions, the first-mode

natural frequencies experienced notable increases when compared to floors under simply supported conditions. Therefore, only considering simply supported conditions at the design stage may lead to an overdesign of the floor. Nevertheless, the current design methods [10,11,19] for controlling the vibration of CLT floors still assume simply supported conditions for estimating fundamental frequency. This assumption will often lead to conservative floor design and unnecessary waste. In fact, the majority of CLT buildings employ platform construction, where each floor is constructed on top of the one below it, so the gravity loads from upper floors transmitted through the floor-to-wall connections will provide a certain level of resistance against rotation at the edge supports [18,20] and will eventually lead to increased natural frequencies.

Besides natural frequencies, the damping ratio is another variable that would be influenced by different boundary conditions. For example, Hamm et al. [21] performed vibration tests on timber floors considering various boundary conditions, including different types of bearings and support configurations (two-sided and four-sided support). Their findings revealed damping ratios ranging from 2.99% to 4.52% under different boundary conditions. Jarnerö et al. [22] considered different simply supported conditions in their vibration tests, and they found that the damping ratio of the floor increases when the floor is placed on an elastic interlayer between the support and the floor. Huang et al. [23] considered the effect of beam space, beam size and supporting conditions on the dynamic behaviours of CLT floors based on a novel model from OPENSEES. They found that the spacing between the supported beams and the supported beams' stiffness have a significant influence on the values of the natural frequency of CLT floors.

Although the studies above highlight the importance of boundary conditions regarding the vibration design of CLT floors, our knowledge of the effect of partially restrained supports in design is still limited. Zhang et al. [20] developed an analytical formula considering end restraint coefficients for various support conditions. The direction of this research is pivotal, as it will provide significant insights for refining existing simplified formulas in current design methods in the future. Theoretically, the factors of frequency constant λ_n can be used to calculate frequencies [17] with different restrained support conditions such as cantilever (C-F), simply supported (S-S), clamped–pinned-supported (C-S) support and clamped–clamped support (C-C). While these factors may not be representative of the actual support conditions, new frequency factors can be extrapolated for various actual support conditions once the inherent properties and vibration frequencies of the tested panels are determined. This concept serves as the foundation of this study.

Therefore, the main objectives of this topic include the following:

- To determine the experimental dynamic responses (fundamental frequency and damping ratio) of *E. nitens* CLT panels under different laboratory-designed support conditions.
- To compare the experimental results of *E. nitens* CLT panels with spruce CLT panels under different laboratory-designed support conditions.
- To determine the frequency constant (λ_1) for different laboratory-designed support conditions based on the experimental results of fundamental frequency and compare them with the theoretical values.

2. Materials and Methods

In this study, cross-laminated timbers (CLTs) constructed from fibre-managed *E. nitens* were the main tested materials, and a controlled CLT made from strength-class C24 spruce [16] was also included for the purpose of comparison. The vibration tests, consisting of a basketball dropped from a known height and an accelerometer, were performed to determine the dynamic response of the CLT panels under three support conditions. The values of fundamental frequency and damping ratio were the main parameters in this study. Theoretical methods were used to determine the frequency constant for different support conditions.

2.1. Materials

The sawn boards were finished to 33 mm × 100 mm (depth × width) before CLT manufacturing. Each CLT panel includes three layers: the outer layers consist of three adjacent sawn boards, and the inner layer consists of twenty adjacent sawn boards. It is important to note that only face-glueing was considered in this study. Seven three-layered CLT panels with nominal dimensions of 100 mm × 300 mm × 2000 mm (thickness × width × length) were fabricated by CUSP Building Solutions, Wynyard, Tasmania, Australia. Six of them were made from fibre-managed *E. nitens* sawn boards, which were graded by non-destructive four-point bending tests before CLT manufacturing. The *E. nitens* feedstocks were then divided into three groups by sorting them into high MOE (H), medium MOE (M) and low MOE (L). The ranges of MOE for each group are summarised in Table 1.

Table 1. MOE ranges of sawn boards.

Species	Groups	MOE Range (GPa)	Average MOE ± StdDev (GPa)	Average Density ± StdDev (kg/m ³)
<i>E. nitens</i> (EN)	High MOE	11.9–14.8	13.2 ± 0.8	560.7 ± 49.0
	Medium MOE	9.6–11.6	10.6 ± 0.7	513.0 ± 33.7
	Low MOE	8.0–8.7	8.4 ± 0.2	491.6 ± 41.9
Spruce sawn boards		11.0 ¹	-	414.6 ± 18.0

¹ The spruce sawn boards were graded by industry experts and classified as strength-class C24 based on standard EN 338 [16].

Two heterogeneous, three-layered CLT configurations using material from different MOE groups in different layers (EN-HLH and EN-MLM) and one homogeneous configuration (EN-MMM) were manufactured. The wood grain direction was aligned with the beam axis for the top and bottom layers and transversely for the middle layer. Each configuration had two replicates. The intent of the EN-HLH and EN-MLM configurations was to maximise the use of lower-grade material where it was not critical while still achieving good stiffness through the use of a higher MOE in the outer layers. In addition, one spruce CLT panel was included as a control reference, acting as a benchmark for comparing the experimental results.

All CLT panels were subjected to non-destructive four-point bending tests to measure their apparent MOE and bending stiffness (EI). The testing setup followed the procedures outlined in Australian Standard AS/NZS 4063.1 [24], and the MOE values are calculated by Equation (1). This setup included a span length equal to 18 times the thickness of the samples, supported by two roller supports. Then, an LVDT was employed to measure the mid-span deflection as the panels were subjected to loads applied by a loading frame with two-point loads. The loading process for each CLT panel was stopped before reaching the span limit of the deflection (6 mm in this case). These properties are important for the calculations in this study (Table 2) and were determined by a previous study [15].

$$\text{MOE} = \frac{23L^3 \Delta F}{108bd^3 \Delta e} \quad (1)$$

where MOE is the modulus of elasticity of the tested samples in MPa, L is the span length between two supports in mm, d is the thickness of the tested samples in mm and $\Delta F/\Delta e$ is the slope of the load-deflection curve in the linear-elastic range.

Table 2. Mean density, apparent MOE and bending stiffness of CLT panels.

CLT Configurations	Mean Density (kg/m ³)	Apparent MOE (GPa)	EI (N·m ² × 10 ⁵)
EN-HLH1	519.1	11.7	3.0
EN-HLH2	545.5	11.5	3.0
EN-MLM1	519.1	9.1	2.3
EN-MLM2	521.0	9.0	2.3
EN-MMM1	498.4	9.3	2.4
EN-MMM2	515.8	9.5	2.5
Spruce CLT	413.7	8.3	2.0

2.2. Impact Response Tests

In residential buildings, vibrations and the consequent noise caused by footsteps are the major source of human discomfort and often manifest as short-term transient oscillations. Hence, several studies have conducted vibration tests of floors by employing real footfalls as the excitation source [23,25–27]. However, assuming that for small-amplitude vibrations the response is linear, the response of the floor to a footfall can be obtained by convolution of the temporal profile of a footfall with the impulse response of the floor. Thus, the essential information about the flooring system can be obtained through impulse-response testing, which affords more controlled experiments and yields cleaner responses in terms of both frequency and damping ratios. The typical techniques to test the dynamic responses of timber floors described in the literature include brushing the OSB floors [28], punching with the fist against the bottom of the timber floors [21] and dropping a basketball on nail-laminated timbers [29].

In this study, the vibration tests were conducted using a 600 g basketball and an accelerometer. Five impact locations were marked on the surface of each panel, and each location was spaced 300 mm apart. The supported regions of the CLT panels were vibration nodes (locations of zero motion); hence, they were not included as impact locations (Figure 1). Each impact location was subjected to 3 excitations by dropping a basketball from a consistent height of 300 mm, so a total of 15 measurements were included for each CLT sample under each support condition. In addition, the accelerometer was secured to the bottom mid-span of the panel. This position allowed for more impact locations and prevented any interference with the accelerometer caused by the basketball drops. In this study, only the fundamental frequencies (first-mode natural frequency) were considered. That is because the fundamental frequencies are usually the lowest compared to other bending mode shapes.

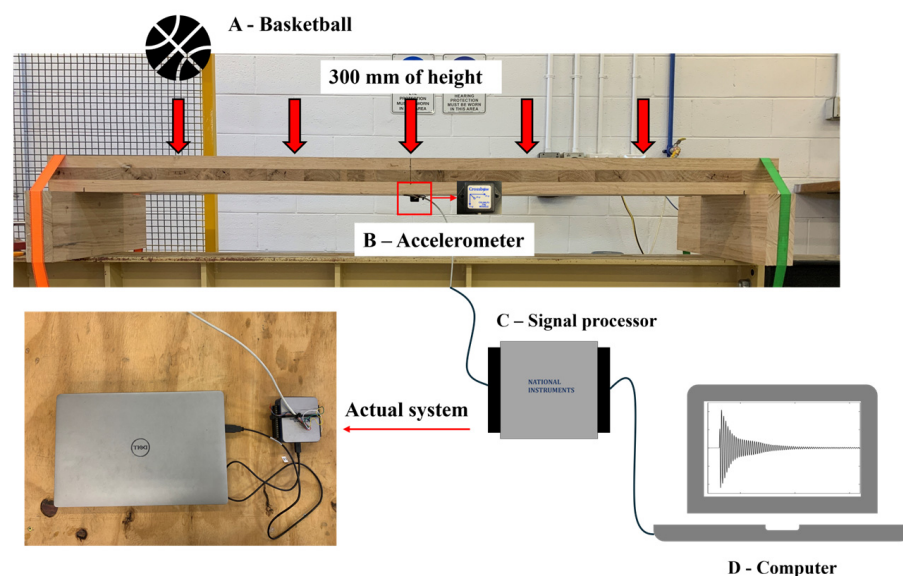


Figure 1. Impact response tests and data acquisition system.

The data acquisition system included four main parts (Figure 1). A 600 g basketball (A) was used as an excitation source by dropping it from a consistent height of 300 mm. Then, a Crossbow CXL04LP3 accelerometer (B) with a sensitivity of 500 ± 25 mV/g was employed to measure the vertical acceleration-time data, sampled at a frequency of 6000 Hz. A signal processor (C) was included to interpret the output data from the accelerometer, and then the output data were recorded as a CSV file by National Instruments LabVIEW version 15.0.1 on a computer (D). The data were then analysed by Fast Fourier Transformation (FFT) in MATLAB R2021b. The impact response test used in this study was similar to the procedure mentioned in ISO 18324:2016 [30].

Three support conditions were considered in this study: roller–roller support (Figure 2a), bearer–bearer support (Figure 2b) and clamp–bearer support (Figure 2c). The clamp-and-bearer support conditions were intended to model supports that would replicate conditions in a real structure more realistically. The spans of the supports were 2 m for the roller–roller support and 1.93 m for the bearer–bearer and clamped–bearer supports (the thickness of the bearer was 70 mm).

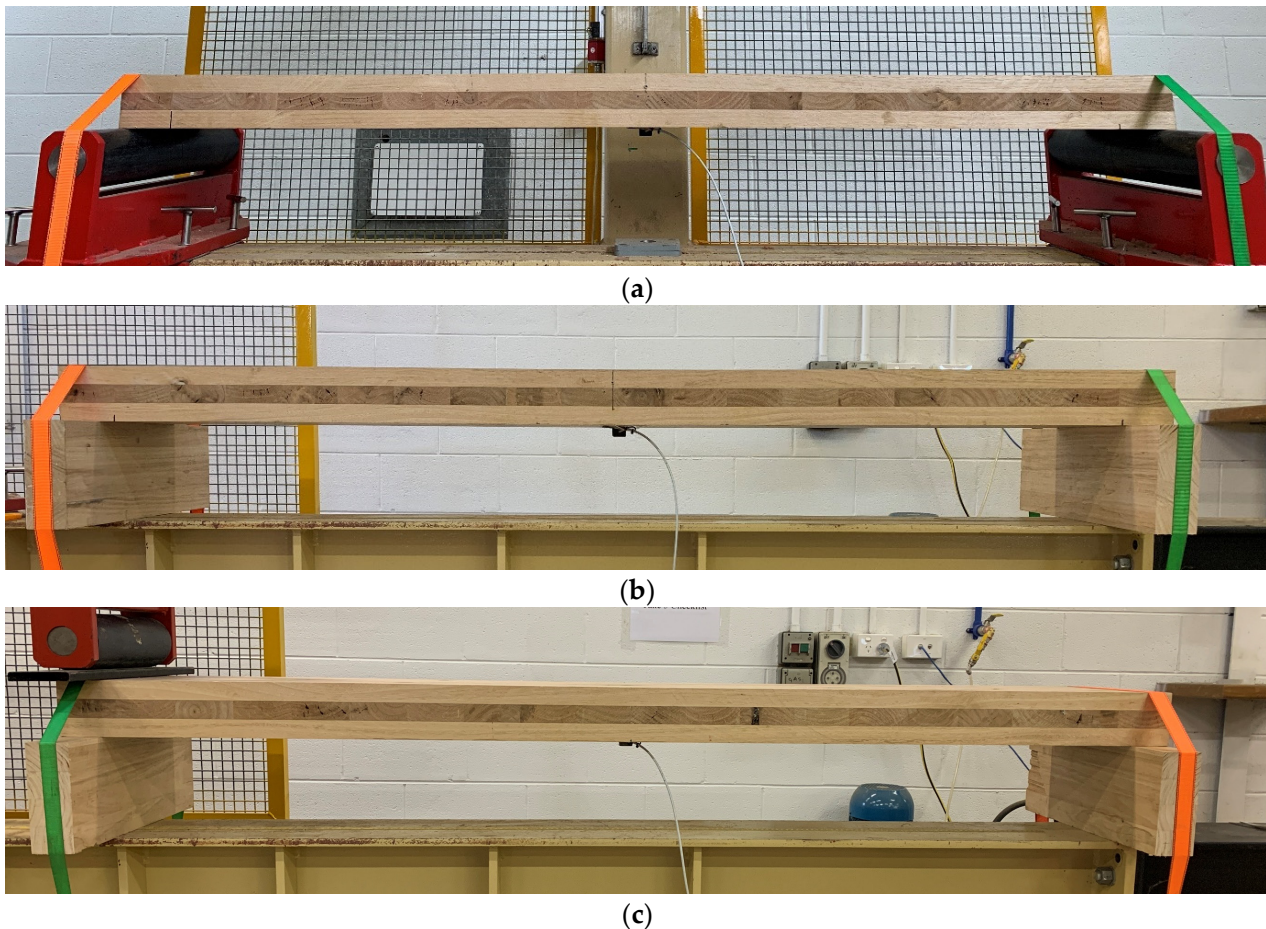


Figure 2. Setups of support conditions: (a) roller–roller support; (b) bearer–bearer support; (c) clamped–bearer support with three different clamping loads.

At each end of the support, a ratchet strap was employed to secure the panels. The purpose of the ratchet straps was to prevent the panel from rebounding upward when subjected to the excitation of a dropping basketball, but the vertical force may also alter the effective stiffness of the bearer and roller supports, which were not necessarily ideal simple supports (this is discussed further later). For the clamped end condition, three different levels of loads were applied by the CALIBRE bending rig (4.91 kN, 7.36 kN and 9.81 kN). The loading process was stopped immediately by the LabView version 13.0f1 on the computer once the desired loads were achieved.

2.3. Data Analysis

2.3.1. Fundamental Frequency and Damping Ratio

The time-domain signal was transformed into frequency-domain data (Figure 3) for the purpose of determining the natural frequency using Fast Fourier Transformation (FFT), which is an effective method for calculating discrete Fourier transforms (DFTs) [31].

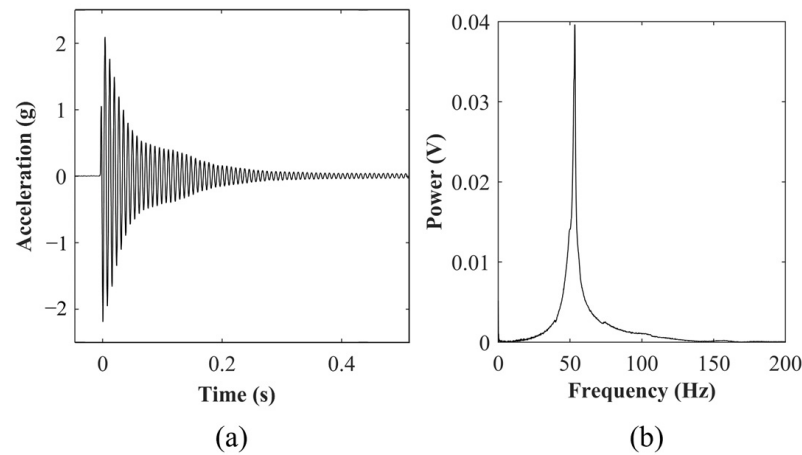


Figure 3. (a) Typical acceleration-time graph; (b) frequency response spectrum.

The damping ratio was determined from the time-domain signal. In the time domain, the damped vibration following the impulse can be approximated by the following general equation [17]:

$$x = Xe^{-\zeta\omega t} \sin\left(\sqrt{1 - \zeta^2}\omega t + \varphi\right) \quad (2)$$

where ζ is the damping ratio (%), ω is the undamped circular frequency (rad/sec) (the undamped natural frequency and the damped natural frequency for a system with light damping can be assumed to be the same, e.g., if $\zeta = 3\%$, then $\sqrt{1 - \zeta^2}\omega = 0.9995\omega$), t is time (s) and X and φ are the initial condition-defined arbitrary phase and amplitude constants.

The amplitude of the oscillations is controlled by the exponential term shown in Equation (3):

$$y = Xe^{-\zeta\omega t} \quad (3)$$

Then, the curve fitting function from MATLAB R2021b was used to match the maxima from the acceleration-time data with Equation (4) (Figure 4a).

$$f(t) = ae^{bt} \quad (4)$$

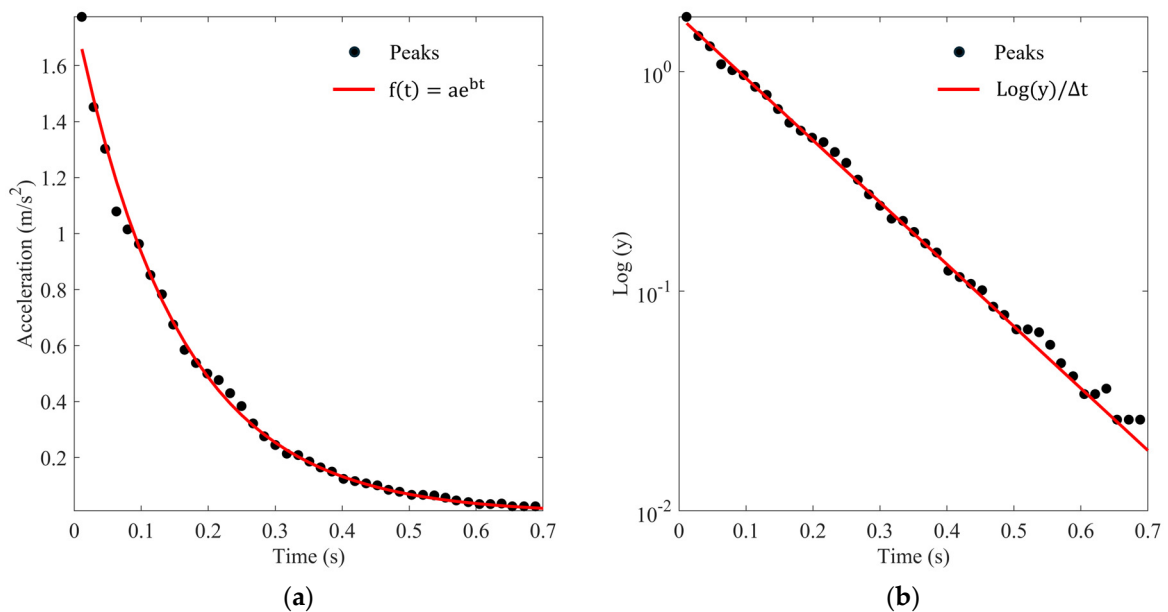


Figure 4. (a) Exponential curve fitting; (b) logarithmic decrement.

The value of the damping ratio can be estimated by Equation (5):

$$\zeta = \frac{b}{\omega} = \frac{b}{2\pi f} \quad (5)$$

where a and b are constant parameters and f is the undamped natural frequency (Hz).

In addition, the logarithmic decrement method was also applied by differentiating and rearranging Equation (3):

$$\zeta = -\frac{1}{\omega} \frac{d(\log(y))}{dt} \approx \frac{1}{\omega} \frac{\log\left(\frac{y_1}{y_2}\right)}{t_2 - t_1} \quad (6)$$

where y_1 and y_2 are the amplitudes determined at t_1 and t_2 , respectively, between which the relationship $\log(y)$ and t is linear.

Figure 4 shows the typical graphs for calculating the damping ratio.

2.3.2. Determination of Frequency Constant for Different Supported Conditions

The CLT panels in this study could be assumed to be uniform beams due to their narrow width. Hence, the values of the theoretical natural frequency can be determined by the following equation:

$$f_n = \frac{\lambda_n}{2\pi} \sqrt{\frac{EI}{ml^4}} \quad (7)$$

where λ_n are numerical values for end conditions for the n th mode (in this study, only first-mode was considered), EI is the bending stiffness ($\text{N}\cdot\text{m}^2$) as shown in Table 2, m is the mass (kg/m) and l is the span (m).

Then, the experimental values of λ_1 were determined by extrapolating Equation (7), using the experimental results of fundamental frequency, bending stiffness and density (Table 1) and span length.

3. Results

3.1. Results of Fundamental Frequency

The experimental results of the fundamental frequency are summarised in Table 3.

Table 3. Results of fundamental frequency.

Panel Code	Panel No.	Natural Frequency (Hz) \pm StdDev				
		Roller-Roller	Bearer-Bearer	Clamp-Bearer		
				16.4 kN/m	24.5 kN/m	32.7 kN/m
EN-HLH	1	53.2 \pm 0.08	59.1 \pm 0.05	61.2 \pm 0.04	62.1 \pm 0.05	62.9 \pm 0.05
	2	52.4 \pm 0.05	57.9 \pm 0.05	60.4 \pm 0.03	60.8 \pm 0.03	61.1 \pm 0.05
	<i>Average</i>	52.8 \pm 0.37	58.5 \pm 0.59	60.8 \pm 0.41	61.5 \pm 0.67	62.0 \pm 0.92
EN-MLM	1	48.2 \pm 0.00	55.0 \pm 0.05	58.6 \pm 0.05	58.8 \pm 0.05	59.0 \pm 0.07
	2	46.6 \pm 0.07	52.3 \pm 0.06	58.4 \pm 0.04	58.5 \pm 0.04	58.5 \pm 0.04
	<i>Average</i>	47.4 \pm 0.83	53.7 \pm 1.38	58.5 \pm 0.11	58.7 \pm 0.17	58.8 \pm 0.26
EN-MMM	1	46.8 \pm 0.06	54.4 \pm 0.37	55.9 \pm 0.03	56.9 \pm 0.06	57.2 \pm 0.04
	2	47.3 \pm 0.07	54.2 \pm 0.00	57.3 \pm 0.05	57.4 \pm 0.04	58.0 \pm 0.44
	<i>Average</i>	47.1 \pm 0.23	54.3 \pm 0.28	56.6 \pm 0.72	57.2 \pm 0.27	57.6 \pm 0.51
Spruce	1	48.4 \pm 0.15	54.6 \pm 0.05	56.8 \pm 0.06	57.2 \pm 0.04	57.2 \pm 0.07

3.2. Results of Damping Ratio

The experimental results of the damping ratio calculated by the logarithmic decrement method are summarised in Table 4, and the comparison of results between the exponential decay curve fitting and the logarithmic decrement method is included in Table 5.

Table 4. Results of damping ratio using logarithmic decrement method.

Panel Code	Panel No.	Damping Ratio (%) \pm StdDev				
		Roller–Roller	Bearer–Bearer	Clamp–Bearer		
				16.4 kN/m	24.5 kN/m	32.7 kN/m
EN-HLH	1	2.1 \pm 0.12	1.8 \pm 0.02	1.7 \pm 0.04	1.6 \pm 0.04	1.5 \pm 0.05
	2	1.9 \pm 0.07	2.2 \pm 0.11	1.2 \pm 0.12	1.3 \pm 0.03	1.2 \pm 0.05
	<i>Average</i>	2.0	2.0	1.4	1.4	1.3
EN-MLM	1	2.1 \pm 0.06	1.7 \pm 0.02	1.6 \pm 0.11	1.5 \pm 0.05	1.5 \pm 0.05
	2	2.5 \pm 0.31	2.8 \pm 0.18	2.3 \pm 0.13	2.4 \pm 0.15	2.3 \pm 0.09
	<i>Average</i>	2.3	2.2	2.0	1.9	1.9
EN-MMM	1	1.5 \pm 0.02	2.6 \pm 0.07	2.6 \pm 0.13	2.3 \pm 0.06	2.1 \pm 0.10
	2	2.2 \pm 0.06	2.4 \pm 0.07	1.9 \pm 0.04	1.8 \pm 0.05	1.9 \pm 0.05
	<i>Average</i>	1.9	2.5	2.2	2.1	2.0
Spruce	1	2.8 \pm 0.15	3.0 \pm 0.07	1.8 \pm 0.05	1.6 \pm 0.08	1.7 \pm 0.11

Table 5. Comparison between exponential curve fitting and logarithmic decrement method.

CLT Configurations	Damping Ratio (%)									
	Roller–Roller		Bearer–Bearer		Clamp–Bearer					
					16.4 kN/m		24.5 kN/m		32.7 kN/m	
	exp.	log.	exp.	log.	exp.	log.	exp.	log.	exp.	log.
EN-HLH	2.1	2.0	1.8	2.0	1.4	1.4	1.4	1.4	1.3	1.3
EN-MLM	2.2	2.3	2.2	2.2	1.8	2.0	1.8	1.9	1.8	1.9
EN-MMM	2.0	1.9	2.8	2.5	2.2	2.2	2.2	2.1	2.2	2.0
Spruce	2.7	2.8	3.0	3.0	1.7	1.8	1.7	1.6	1.8	1.7

3.3. Results of Frequency Constant for Different Support Conditions

The results of the frequency constant (λ_1) determined by extrapolating Equation (7) are summarised in Table 6.

Table 6. Results of frequency constant (λ_1).

Panel Code	Panel No.	Frequency Constant (λ_1)				
		Roller–Roller	Bearer–Bearer	Clamp–Bearer		
				16.4 kN/m	24.5 kN/m	32.7 kN/m
EN-HLH	1	9.6	10.0	10.3	10.5	10.6
	2	9.8	10.1	10.5	10.6	10.6
	<i>Average</i>	9.7	10.0	10.4	10.5	10.6
EN-MLM	1	9.9	10.5	11.2	11.3	11.3
	2	9.6	10.0	11.1	11.2	11.2
	<i>Average</i>	9.7	10.3	11.2	11.2	11.2
EN-MMM	1	9.3	10.1	10.3	10.5	10.6
	2	9.4	10.1	10.6	10.7	10.8
	<i>Average</i>	9.4	10.1	10.5	10.6	10.7
Spruce	1	9.6	10.0	10.4	10.5	10.5
Overall Average		9.6	10.1	10.7	10.7	10.8
CV* (%)		2.1	1.9	3.5	3.1	2.9

* CV represents the coefficient of variation.

4. Discussion

4.1. Fundamental Frequency

For the results of fundamental frequency (Table 3), EN-HLH CLT exhibited the highest values across all supported conditions. In addition, EN-MLM and EN-MMM CLTs yielded comparable results to each other. Bending stiffness (EI) and mass (density) are important factors for determining the fundamental frequency of vibration. It should be noted that, due to the cross-lamination layup, the middle layer of CLT contributes only around 0.38% to the bending stiffness, due to the fact that the MOE in the radial and tangential directions is around 1/10th that of the longitudinal direction. Therefore, although the middle layer of EN-MLM has around 20% less MOE compared to EN-MMM, this difference does not significantly affect the bending stiffness of CLT and eventually influences the results of fundamental frequency, as the values of density of *E. nitens* CLT (Table 2) are also relatively similar.

The controlled spruce CLT panel exhibits around 7.7% lower fundamental frequency results than EN-HLH CLT panels across all support conditions, while showing comparable results to EN-MLM and EN-MMM CLT panels. The spruce CLT panel has the lowest bending stiffness and density (Table 2) among all CLT panels. According to Equation (7), lower bending stiffness would lead to lower values of fundamental frequency; however, lower mass (density) would result in higher values of fundamental frequency. In this study, spruce CLT has around 9.8% lower bending stiffness compared to EN-MLM and EN-MMM CLT panels, while it has around 19.4% lower density than EN-MLM and EN-MMM CLT panels. Based on the observations in this study, EN-MLM and EN-MMM CLT panels showed around 2% lower fundamental frequency results than spruce CLT under simply supported conditions (roller–roller and bearer–bearer), while they showed approximately 1.5% higher fundamental frequency results than spruce CLT under clamped–bearer conditions.

In this study, the roller–roller support condition was designed to simulate the theoretical simply supported condition, since this is a well-defined condition. However, this setup may not fully capture the situation in practical buildings, which include bearers and walls to contribute nominally rigid moment connections. Through the comparison of fundamental frequencies between the roller–roller and bearer–bearer support conditions, the latter condition shows 11.5% higher average results than the former one. The higher results may be attributed to a combination of factors, including the reduction in span and increased end restraint. Furthermore, a slightly increasing trend in the values of fundamental frequency was found when the applied load at the edge of the CLT panels was increased under clamp–bearer support conditions. Further information related to the values of the frequency constant (λ_1) for different support conditions will be discussed in Section 4.3.

4.2. Damping Ratio

In this study, two methods were used to calculate the damping ratio. Generally, the logarithmic decrement method can be considered more reliable. That is because, firstly, the curve fitting method may be significantly influenced by the much larger values at earlier times, which are likely to be inaccurate because of the possibility of the presence of multiple modes being excited; and secondly, when the peaks are plotted on a log axis (Figure 4b), it is obvious whether the assumption of linearity has been met. However, there is excellent agreement between these two methods in this study, with maximum differences of about 10%, which is within the measurement uncertainty (Table 5), so both methods may be regarded as accurate. The results of the damping ratio (Table 4) did not reveal any obvious correlation with either the *E. nitens* CLT configurations or the feedstock species employed. However, the results of the damping ratio showed an obvious reducing trend when clamping loads were applied. Taking spruce CLT as an example, the damping ratios dropped by around 75% once clamping loads were applied. The phenomenon of decreasing damping ratio under clamped edge conditions was also observed in a previous study conducted by Weckendorf et al. [32]. In addition, the values of the damping ratio

slightly decreased when the applied loads increased. This may suggest that increasing the applied loads at the edge support would decrease the structural damping because it provides a lower opportunity for slippage and friction.

It is worth noting that damping ratios measured in laboratory settings are often significantly lower than those determined in actual construction scenarios. The reason for this discrepancy may be the installation of the system in a real structure, which would lead to an increase in energy loss through various connections. The damping would also be significantly affected by different construction techniques and the quality of workmanship [33]. While the damping ratio values in this study may not precisely replicate real-world scenarios, understanding the evolving trend of damping ratio across different end restraint conditions may provide valuable insights into how CLT panels can effectively achieve the desired vibrational performance in practical situations.

4.3. Frequency Constant λ_1

For the CLT configurations and wood species, the variation in the frequency constant (λ_1) was small (average CV of less than 3%) under the same support conditions (Table 6). This suggested that the experimental results of fundamental frequency reflected the properties (bending stiffness and density) of all CLT samples well. However, the values of λ_1 varied based on different support conditions.

According to the theory of Euler Equation for Beams, the theoretical values of frequency constant λ_1 for ideal simply supported (S-S) and clamped–pinned supported (C-S) supports can be summarised as the values in Table 7 [17].

Table 7. Theoretical values of λ_1 for different end conditions.

End Conditions	Numerical Values (λ_1)
Simply supported	9.87
Clamped–pinned	15.4

The average values of λ_1 (Table 6) for roller–roller and bearer–bearer supports align closely with the theoretical λ_1 values (Table 7). To be more detailed, the values of λ_1 for roller–roller support are 2.7% lower, while the values of λ_1 for bearer–bearer support are 2.3% higher, when compared to the theoretical λ_1 under the ideal simply supported end condition. It is crucial to note that some standards and handbooks, such as Eurocode 5 [34] and the Canadian CLT Handbook [10], have accepted the theoretical λ_1 values for simply supported conditions to estimate the fundamental natural frequency of timber/CLT floors. The closely aligned results observed in this study may suggest that the existing method for determining the fundamental frequency of timber floors may be applicable for CLT floors made from fibre-managed *E. nitens*; however, further considerations would be required and will be discussed in Section 4.4.

In addition, the values of λ_1 increased by 5.6% when one edge of the bearer–bearer support was subjected to edge loads (16.4 kN/m) by the bending rig (Figure 2c). When the edge loads increased, the values of λ_1 increased slightly (this was not obvious when the edge loads increased from 16.4 kN/m to 24.5 kN/m, but the values increased by around 1% when the edge loads increased to 32.7 kN/m). This finding aligned closely with the previous study conducted by Zhang and Chui [35], who investigated the influence of end support restraints on the vibration performance of SPF CLT panels considering different top loads at the end supports.

Although the values of λ_1 experienced an increasing trend when clamping loads were applied, the values were still far below the theoretical λ_1 (Table 7) for ideal clamped–pinned (C-S) support. In practical situations, clamping conditions may be referred to as floor-to-wall connections. However, the results of this study indicated that the experimental clamped condition was not 100% effective in preventing rotation. Also, it is likely that real structures do not provide perfectly rigid end restraints on walls. Therefore, considering

the partially restrained effect on the vibration performance of CLT panels is essential for design assessment. In addition, it is highly suggested that the approximate formula for the estimation of the natural frequency of CLT floors used in design methods [10,11,19] should accommodate different factors corresponding to various end restraint conditions. While the λ_1 values in this study may not fully reflect the real-world support conditions in practice, the significance of the ongoing research on *E. nitens* CLT connections continues to grow. Therefore, investigating the vibration characteristics of *E. nitens* CLT under various actual end restraint conditions will emerge as a pivotal step in this research domain. This study laid the groundwork for future investigations in this direction.

4.4. Research Limitations

In this study, the CLT panels are beam-like samples, and the results obtained would be more representative of situations when the panels are used as beams or floors supported by two edges. However, when CLT floors exhibit plate-like behaviour and are supported on all four sides, the dynamic responses will be totally different. That is because, when side edges are restrained, additional stiffness in the whole system will be introduced, which will lead to an increase in the fundamental natural frequency. According to the research conducted by Ussher et al. [36], the first-mode natural frequency increases around four times when the boundary conditions of the five-ply single CLT plate transit from SFSF to SSSS. Therefore, the estimations of vibration for beam-like CLT may be conservative.

5. Conclusions

This study has investigated the influence of different support conditions on the vibration serviceability performance of hardwood CLT panels with a combination of different grades in panel laminations from fast-grown plantation *E. nitens* timber boards. The following are the key findings of this research:

- The results of the fundamental frequency were mostly influenced by the grade of the *E. nitens* boards used in the outer layers (average of 13.2 GPa for high MOE and 10.6 GPa for medium MOE), while the grade of *E. nitens* in the inner layers (average of 10.6 GPa for medium MOE and 8.4 for low MOE) had a minor influence on the fundamental frequency due to the lesser generation of stiffness in the whole CLT panels.
- Spruce CLT has around 9.8% lower bending stiffness compared to EN-MLM and EN-MMM CLT panels, while it has around 19.4% lower density than EN-MLM and EN-MMM CLT panels. Therefore, EN-MLM and EN-MMM CLT panels showed fundamental frequency results that were comparable to those of the controlled spruce CLT across all support condition setups. While spruce has been widely used in CLT production, the design criteria regarding frequency-domain analysis that have been used in spruce CLT may be applicable to *E. nitens* CLT.
- No apparent relationship was observed in the damping ratio of vibration among CLT panels made from different configurations and species.
- The values of frequency constant λ_1 for the roller–roller (average of 9.6) and bearer–bearer (average of 10.1) support conditions are aligned with the theoretical values (9.87) for simply supported end conditions.
- The values of frequency constant λ_1 for clamp–bearer support remain far below the theoretical values for clamped–pinned support, even with an increase in clamping loads up to 32.7 kN/m. It should be noted that achieving absolute clamping conditions under laboratory conditions or through end restraints provided by walls in real structures may not be feasible. However, there is a slight increasing trend observed when edge loads increase. This may hint at the fact that the lower floors in a multi-level building, for example, would have slightly higher fundamental frequency values compared to the upper floors. This is likely due to higher loads applied at the floor edges, stemming from the cumulative load imposed by the upper floors and transmitted through the walls, which are sitting at the edge of the floors.

Author Contributions: Conceptualisation, Y.L. and A.T.; methodology, Y.L.; software, Y.L.; validation, A.T., N.K., A.C. and D.H.; formal analysis, Y.L.; investigation, Y.L.; resources, A.T.; data curation, Y.L.; writing—original draft preparation, Y.L.; writing—review and editing, A.T., N.K., A.C. and D.H.; visualisation, Y.L.; supervision, A.T., N.K., A.C. and D.H.; project administration, A.T.; All authors have read and agreed to the published version of the manuscript.

Funding: This research received no external funding.

Data Availability Statement: Data are contained within the article.

Conflicts of Interest: The authors declare no conflict of interest.

References

1. ABARES. Australian Plantation Statistics and Log Availability Report: October 2021. In *Australian Bureau of Agricultural and Resource Economics and Sciences*; ABARES: Canberra, Australia, 2021.
2. Derikvand, M.; Kotlarewski, N.; Lee, M.; Jiao, H.; Chan, A.; Nolan, G. Visual stress grading of fibre-managed plantation Eucalypt timber for structural building applications. *Constr. Build. Mater.* **2018**, *167*, 688–699. [\[CrossRef\]](#)
3. Balasso, M.; Hunt, M.; Jacobs, A.; O'Reilly-Wapstra, J. Development of Non-Destructive-Testing Based Selection and Grading Strategies for Plantation Eucalyptus nitens Sawn Boards. *Forests* **2021**, *12*, 343. [\[CrossRef\]](#)
4. Ettelaei, A.; Taoum, A.; Nolan, G. Assessment of Different Measurement Methods/Techniques in Predicting Modulus of Elasticity of Plantation Eucalyptus nitens Timber for Structural Purposes. *Forests* **2022**, *13*, 607. [\[CrossRef\]](#)
5. Ettelaei, A.; Taoum, A.; Shanks, J.; Nolan, G. Rolling Shear Properties of Cross-Laminated Timber Made from Australian Plantation Eucalyptus nitens under Planar Shear Test. *Forests* **2022**, *13*, 84. [\[CrossRef\]](#)
6. Pangh, H.; Hosseinabadi, H.Z.; Kotlarewski, N.; Moradpour, P.; Lee, M.; Nolan, G. Flexural performance of cross-laminated timber constructed from fibre-managed plantation eucalyptus. *Constr. Build. Mater.* **2019**, *208*, 535–542. [\[CrossRef\]](#)
7. *ISO 2631-1*; Mechanical Vibration and Shock—Evaluation of Human Exposure to Whole-Body Vibration—Part 1: General Requirements. International Organization for Standardization: Geneva, Switzerland, 1997.
8. *ISO 2031-2*; Mechanical Vibration and Shock—Evaluation of Human Exposure to Whole-Body Vibration—Part 2: Vibration in Buildings (1 Hz to 80 Hz). International Organization for Standardization: Geneva, Switzerland, 2003.
9. Hu, L.J. Serviceability of next generation wood buildings: Laboratory study of vibration performance of cross-laminated-timber (CLT) floors. In *Wood Products*; Canadian Forest Service: Québec, QC, Canada, 2013.
10. Karacabeyli, E.; Gagnon, S. *Canadian CLT Handbook 2019 Edition*; FPInnovations: Pointe-Claire, QC, Canada, 2019; Volume 1.
11. *CSA-O86:19*; Engineering Design in Wood. Canadian Standards Association, National Standard of Canada: Toronto, ON, Canada, 2021.
12. Chuláin, C.U.; Harte, A.M. Experimental investigation of the serviceability behaviour of a cross laminated timber floor. In Proceedings of the Civil Engineering Research in Ireland Conference (CERI 2018), Dublin, Ireland, 30 August 2018.
13. *EN 16929*; Test Methods—Timber floors—Determination of Vibration Properties. European Committee for Standardization (CEN): Brussels, Belgium, 2019.
14. Crovella, P.; Kurzinski, S. Predicting the Strength and Serviceability Performance of Cross-laminated Timber (CLT) Panels Fabricated with High-Density Hardwood. In Proceedings of the World Conference on Timber Engineering (WCTE), Santiago, Chile, 9–12 August 2021.
15. Liang, Y.; Taoum, A.; Kotlarewski, N.; Chan, A.; Holloway, D. Behavior of Cross-Laminated Timber Panels Made from Fibre-Managed Eucalyptus nitens under Short-Term Serviceability Loads. *Buildings* **2023**, *13*, 245. [\[CrossRef\]](#)
16. *EN 338*; Structural Timber—Strength Classes. European Committee for Standardization (CEN): Brussels, Belgium, 2016.
17. Thomson, W.T.; Dahleh, M.D. *Theory of Vibration with Applications*, 5th ed.; Prentice Hall: Hoboken, NJ, USA, 1998.
18. Chuláin, C.U.; Sikora, K.; Harte, A.M. Influence of connection systems on serviceability response of CLT timber flooring. In Proceedings of the World Conference on Timber Engineering WCTE16, Vienna, Austria, 22–25 August 2016.
19. Gustafsson, A.; Crocetti, R.; Just, A.; Landel, P.; Olsson, J.; Pousette, A.; Silfverhielm, M.; Östman, B. *The CLT Handbook: CLT Structures—Facts and Planning*; Swedish Wood: Stockholm, Sweden, 2019.
20. Zhang, S.; Zhou, J.; Niederwestberg, J.; Chui, Y.H. Effect of end support restraints on vibration performance of cross laminated timber floors: An analytical approach. *Eng. Struct.* **2019**, *189*, 186–194. [\[CrossRef\]](#)
21. Hamm, P.; Richter, A.; Winter, S. Floor vibrations—new results. In Proceedings of the World Conference on Timber Engineering (WCTE2010), Trentino, Italy, 20–24 June 2010.
22. Jarnerö, K.; Brandt, A.; Olsson, A. Vibration properties of a timber floor assessed in laboratory and during construction. *Eng. Struct.* **2015**, *82*, 44–54. [\[CrossRef\]](#)
23. Huang, H.; Gao, Y.; Chang, W.-S. Human-induced vibration of cross-laminated timber (CLT) floor under different boundary conditions. *Eng. Struct.* **2020**, *204*, 110016. [\[CrossRef\]](#)
24. *AS/NZS 4063.1*; Characterisation of Structural Timber Test Methods. Standard Australia: Sydney, Australia; Standard New Zealand: Wellington, New Zealand, 2010.
25. Johansson, P. Vibration of Hollow Core Concrete Elements Induced by Walking. Master's Thesis, Lunds Tekniska Högskola, Lunds Universitet, Lund, Sweden, 2009.

26. Wang, C.; Chang, W.-S.; Yan, W.; Huang, H. Predicting the human-induced vibration of cross laminated timber floor under multi-person loadings. *Structures* **2021**, *29*, 65–78. [[CrossRef](#)]
27. Opazo-Vega, A.; Muñoz-Valdebenito, F.; Oyarzo-Vera, C. Damping Assessment of Lightweight Timber Floors Under Human Walking Excitations. *Appl. Sci.* **2019**, *9*, 3759. [[CrossRef](#)]
28. Weckendorf, J.; Zhang, B.; Kermani, A.; Dodyk, R.; Reid, D. Assessment of Vibrational Performance of Timber Floors. In Proceedings of the 9th World Conference on Timber Engineering, Portland, OR, USA, 6–10 August 2006.
29. Taoum, A.; Jiao, H.; Holloway, D.; Shanks, J. Behaviour of locally post-tensioned nail laminated high mass floor panels under serviceability loads. *Aust. J. Struct. Eng.* **2019**, *20*, 115–123. [[CrossRef](#)]
30. *ISO 18324; Timber Structures—Test Methods—Floor Vibration Performance*. International Organization for Standardization: Geneva, Switzerland, 2016.
31. Bergland, G.D. A guided tour of the fast Fourier transform. *IEEE Spectr.* **1969**, *6*, 41–52. [[CrossRef](#)]
32. Weckendorf, J.; Ussher, E.; Smith, I. Dynamic response of CLT plate systems in the context of timber and hybrid construction. *Compos. Struct.* **2016**, *157*, 412–423. [[CrossRef](#)]
33. Dolan, J.; Murray, T.; Johnson, J.; Runte, D.; Shue, B. Preventing annoying wood floor vibrations. *J. Struct. Eng.* **1999**, *125*, 19–24. [[CrossRef](#)]
34. *EN 1995-1-1; Eurocode 5: Design of Timber Structures—Part 1-1: General—Common Rules and Rules for Buildings*. CEN European Committee for Standardization (CEN): Brussels, Belgium, 2004.
35. Zhang, S.; Chui, Y.H. Quantifying the effect of end support restraints on vibration serviceability of mass timber floor systems: Testing. *Eng. Struct.* **2024**, *301*, 117189. [[CrossRef](#)]
36. Ussher, E.; Arjomandi, K.; Weckendorf, J.; Smith, I. Predicting effects of design variables on modal responses of CLT floors. *Structures* **2017**, *11*, 40–48. [[CrossRef](#)]

Disclaimer/Publisher’s Note: The statements, opinions and data contained in all publications are solely those of the individual author(s) and contributor(s) and not of MDPI and/or the editor(s). MDPI and/or the editor(s) disclaim responsibility for any injury to people or property resulting from any ideas, methods, instructions or products referred to in the content.